Available online at www.sciencedirect.com
SCIENCE DIRECT®
C. R. Mecanique 334 (2006) 213–219
COMPTES RENDUS MECANIQUE
http://france.elsevier.com/direct/CRAS2B/

# Stress-based upper-bound method and convex optimization: case of the Gurson material

Franck Pastor [a], Malorie Trillat [b], Joseph Pastor [b,*], Etienne Loute [a]

[a] *Facultés universitaires Saint-Louis, boulevard Jardin Botanique 43, B-1000 Brussels, Belgium*
[b] *Laboratoire « Optimisation de la conception et ingénierie de l'environnement » (LOCIE), bâtiment Chartreuse, campus scientifique, 73376 Le Bourget du Lac, France*

Received 22 July 2005; accepted after revision 10 February 2006

Available online 11 April 2006

Presented by Jean Salençon

**Abstract**

A nonlinear interior point method associated with the kinematic theorem of limit analysis is proposed. Associating these two tools enables one to determine an upper bound of the limit loading of a Gurson material structure from the knowledge of the sole yield criterion. We present the main features of the interior point algorithm and an original method providing a rigorous kinematic bound from a stress formulation of the problem. This method is tested by solving in plane strain the problem of a Gurson infinite bar compressed between rough rigid plates. ***To cite this article: F. Pastor et al., C. R. Mecanique 334 (2006).***


**Résumé**

**Méthode cinématique par les contraintes et optimisation convexe : cas du matériau de Gurson.** Nous proposons une méthode d'optimisation de type point intérieur associée au théorème cinématique de l'analyse limite. L'association de ces deux outils permet de déterminer la borne cinématique du chargement limite d'une structure en matériau de Gurson à partir de la connaissance du seul critère de plasticité. On expose d'abord brièvement la méthode « point intérieur » de résolution d'un problème comportant des conditions linéaires et des conditions non linéaires, puis une formulation originale et rigoureuse, en contraintes, de l'approche cinématique. Cette méthode est validée en résolvant en déformation plane le problème d'une barre en matériau de Gurson comprimée entre deux plateaux rigides rugueux. ***Pour citer cet article : F. Pastor et al., C. R. Mecanique 334 (2006).***


*Keywords:* Porous media; Interior point optimization; Limit analysis; Upper bound method; Gurson material

*Mots-clés :* Milieux poreux ; Optimisation point intérieur ; Analyse limite ; Méthode cinématique ; Matériau de Gurson

* Corresponding author.
*E-mail addresses:* pastor@fusl.ac.be (F. Pastor), joseph.pastor@univ-savoie.fr (J. Pastor).

1631-0721/$ – see front matter 
doi:10.1016/j.crme.2006.03.002

## 1. Introduction

In the matter of ductile failure of porous materials, Gurson's criterion [1] is the most widely accepted because it is based on a homogenization method and on the kinematic approach of limit analysis. Gurson's model treats a hollow von Mises sphere or cylinder with macroscopic strain imposed on the boundary. Recently, in [2], the Gurson model has been validated for a porous material with spherical cavities using both lower and upper-bound methods of limit analysis. The criterion that he proposed for an isotropic matrix containing cylindrical cavities is expressed as follows, in plane strain:

$$\frac{(\sigma_x-\sigma_y)^2+4\sigma_{xy}^2}{4k^2}+2f\cosh\left(\frac{\sigma_x+\sigma_y}{2k}\right)=1+f^2 \tag{1}$$

where $f$ is the porosity rate of the material and $k$ the flow stress in shear or cohesion.

On the other hand, F. Pastor and E. Loute developed an interior point algorithm to solve a general limit analysis problem. These optimization problems present a linear objective function and a mix of linear and nonlinear convex constraints. For problems where the yield criterion is the von Mises one, the nonlinear constraints are convex quadratic inequalities, giving rise to a conic programming problem for which efficient algorithms exist [3]. The Gurson criterion leads to convex inequality constraints which do not fit with the conic programming formulation. An experimental implementation in MATLAB for the case of quadratic inequality constraints, adapted from an algorithm presented by Vial [4] for general convex programming problems, was presented in [5] and improved in [6,7]. These papers focus on solving the plane strain *static* problems of a Mises material and a Gurson material.

The classical solution of the kinematic problem is more complex, in particular in the Gurson case, because the dissipated power rate is not always analytical. In the present Note, this difficulty is circumvented by using a complete stress kinematic formulation requiring only the expression of the yield criterion. This formulation is more general than that of Anderhegen and Knopfel [8] in the case of a linear, continuous velocity field. Furthermore, it is a different, more general formulation than its recent, technical extension by Krabbenhoft et al. [9] in the case of linear, piecewise continuous velocity field, where a velocity discontinuity segment is simulated by means of two (or three in the 3D case) thin finite elements.

## 2. Interior point method and convex optimization

The general form of the optimization problems to solve is as follows, in mathematical notation:

$$\begin{aligned}&\min\ c^Tx\\&\text{s. t. }\ Ax=b\\&\qquad f(x)+s=0\end{aligned} \tag{2}$$

where $c, x\in\mathbb{R}^n$, $b\in\mathbb{R}^m$, $A\in\mathbb{R}^{m\times n}$ is the matrix of the linear constraints, $f=(f_1,\ldots,f_p)$ is a vector-valued function of $p$ quadratic convex numeric functions $f_i$, and $s\in\mathbb{R}_+^p$ is the vector of slack variables associated with these convex constraints. In [6] the $A$ matrix was made full-row rank by using the so-called Cauchy reciprocity conditions, for example in the cases where two diagonals intersect in a square of finite elements, as in Fig. 1. Here, this problem does not exist because the stress variables are only plastically admissible, as will be seen later.

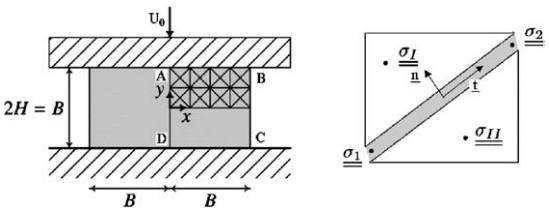


Fig. 1. Left: compression of a bar between rough rigid plates. Right: a discontinuity line.

The primal-dual IP method consists in solving, instead of the previous problem, a series of the following problems, parametrized by decreasing $\mu > 0$, the barrier parameter:

$$\begin{aligned} &\min\ c^T x - \mu \textstyle\sum_{i=1}^{p} \ln(s_i) \\ &\text{s. t. } Ax = b \\ &\qquad f(x) + s = 0 \end{aligned} \tag{3}$$

It can be proved that (3) admits a solution if and only if the KKT conditions are satisfied:

$$\begin{aligned} &c + A^T w + \left(\frac{\partial f}{\partial x}\right)^T y = 0 \\ &Ax - b = 0 \\ &f(x) + s = 0 \\ &YSe = \mu e \end{aligned} \tag{4}$$

where $w \in \mathbb{R}^m$, $y \in \mathbb{R}^p$, $Y$, $S$ are the diagonal matrices associated with $y$ and $s$ respectively, and $e$ is a vector of 1. $\mu > 0$ and $s > 0$ imply $y > 0$. In other words: $f$ are the convex nonlinear yield criteria, $w$ the dual variables associated with the linear constraints and $y$ the dual variables associated with the yield criteria.

After solving a finite series of these problems, with $\mu$ going to 0 in a well-chosen manner, the solution of (2) is approached as closely as needed. Indeed, when $\mu$ approaches zero, Eqs. (4) become close to the KKT conditions for the original problem. The interior point solution of such a system is detailed in [6] and [7] in the static case of limit analysis.

## 3. Limit analysis: a stress-based kinematic method

Now, mechanical notations are used. According to Salençon [10], a stress field $\underline{\underline{\sigma}}$ is said to be admissible if it is statically admissible (SA), i.e., equilibrium equations, continuity and stress boundary conditions are verified, and plastically admissible (PA), i.e. $f(\underline{\underline{\sigma}}) \leqslant 0$ where $f(\underline{\underline{\sigma}}) = 0$ is the (convex) plasticity criterion of the material. In the same way, a strain rate field $\underline{\underline{v}}$ is admissible if it is kinematically admissible (KA), i.e., derived from a piecewise continuous velocity field $\underline{u}$ with bounded discontinuities $[\underline{u}]$ and such that the velocity boundary conditions are verified (in this case $\underline{u}$ will be said also KA), and plastically admissible (PA), i.e., the associated flow rules (6.i), (6.ii) are verified.

Let us assume that the virtual power rate of the external loads $P^{\star}_{\text{ext}}$ can be written as a scalar product of a load vector $\underline{Q}^{\star}$ and a generalized velocity vector $\underline{q}(\underline{u})$. Following [8], the principle of virtual powers states that the stress fields $\underline{\underline{\sigma}}^{\star}$, $\underline{T}^{\star}$ and the load vector $\underline{Q}^{\star}$ are in equilibrium, if for any KA $\underline{u}$ the following variational equation is verified:

$$P^{\star}_{\text{ext}} = \underline{Q}^{\star} \cdot \underline{q}(\underline{u}) = \int_V \underline{\underline{\sigma}}^{\star} : \underline{\underline{v}}\, \mathrm{d}V + \int_{S_d} \underline{T}^{\star}.[\underline{u}]\, \mathrm{d}S \tag{5}$$

In relation (5), $V$ is the volume of the mechanical system, $S_d$ is the union of the velocity discontinuity surfaces. The results in terms of $\underline{Q}^{\star}$ will be interpreted as a kinematical upper bound if, in the corresponding points of $V$, the variables verify the following conditions, where $\underline{q}^d$ is a fixed value of $\underline{q}$:

$$\underline{\underline{v}} = \lambda \frac{\partial f}{\partial \underline{\underline{\sigma}}^{\star}}, \quad f(\underline{\underline{\sigma}}^{\star}) = 0, \quad \lambda \geqslant 0 \tag{6.i}$$

$$[\underline{u}] = \xi \frac{\partial f_{nt}}{\partial \underline{T}^{\star}}, \quad f_{nt}(\underline{T}^{\star}) = 0, \quad \xi \geqslant 0 \tag{6.ii}$$

$$\underline{q}(\underline{u}) = \underline{q}^d \tag{6.iii}$$

The criterion $f_{nt}(\underline{T})$ results from the projection of the plasticity criterion $f(\underline{\underline{\sigma}})$ on the Mohr plane $(\sigma_n, \sigma_{nt})$, where $\underline{n}$ is the normal to the element of the discontinuity surface, and $\underline{T}$ is the stress vector on this element.

It is worth noting that, if relations (6.i), (6.ii) are verified, the quantities $\underline{\underline{\sigma}}^{\star} : \underline{\underline{v}}$ and $\underline{T}^{\star}.[\underline{u}]$ become the corresponding, *convex,* unit dissipated power rates $\pi_V(\underline{\underline{v}})$ and $\pi_d([\underline{u}])$ of LA.

For the sake of simplicity, we assume (without generality loss) that the loading vector of the problem is a scalar, imposed pressure $Q^\star$ (we will examine the case of an imposed velocity later). We will show that relations (6.i) are verified when solving the following problem using the Section 2 algorithm:

$$\text{Max } Q^\star \tag{7.i}$$

$$[\alpha]\{\sigma^\star\} - \{\beta\}Q^\star = 0 \tag{7.ii}$$

$$f(\underline{\underline{\sigma}}^\star) \leqslant 0, \quad \underline{\underline{\sigma}}^\star \text{ is constant inside the finite elements} \tag{7.iii}$$

$$f_{nt}(\underline{T}^\star) \leqslant 0 \quad \text{at the ends of the discontinuity segments} \tag{7.iv}$$

$$+ \text{ KA velocity conditions} \tag{7.v}$$

### *3.1. Case of the virtual continuous velocity field*

Here we use the numerical notation. The virtual, continuous velocity field $\{u\}$ is taken as linearly varying on the $it$ triangular finite element of $S_{it}$ area. Let us consider $\{\sigma^\star\}$ a PA stress field constant on the finite elements. From its definition, writing the external power rate $P^\star_{\text{ext}}$ as $q\,Q^\star = \{u\}^T\{\beta\}Q^\star$ and using the classical FEM relation $\{v\} = [B]\{u\}$ for the $nt$ elements assembling, the equalities in (5) become:

$$P^\star_{\text{ext}} = \sum_{it=1}^{nt} \{v_{it}\}^T\{\sigma^\star_{it}\}S_{it} = \sum_{it=1}^{nt} \{u_{it}\}^T\big[B^T_{it}\big]S_{it}\{\sigma^\star_{it}\} = \{u\}^T[\alpha]\{\sigma^\star\} = \{u\}^T\{\beta\}Q^\star \tag{8}$$

Finally:

$$\{u\}^T\big[[\alpha]\{\sigma^\star\} - \{\beta\}Q^\star\big] = 0 \tag{9}$$

which is the basis of the above (7.ii) equations.

Let us consider now the solution of problem (2), with $A = [[\alpha], -\{\beta\}]$, $b = 0$, $x^T = \{\{\sigma^\star\}^T, Q^\star\}$, the sign of the $c$ functional coefficients being changed because of the present maximization. The *optimal* primal-dual solution $(\{w\}, \{y\}, \{\sigma^\star\}, Q^\star)$ of this problem verifies equations (4) with $\mu e = 0$, i.e., $y_{it} \geqslant 0$ if $f(\underline{\underline{\sigma}}_{it}) = 0$, null otherwise. After transposition, the first equation of (4) becomes:

$$-\{c\}^T + \{w\}^T\big[[\alpha], -\{\beta\}\big] + \{y\}^T\left\{\frac{\partial f}{\partial \sigma^\star}\right\} = 0 \tag{10}$$

Identifying $-\{w\}^T$ as $\{u\}^T$, we note:

- the $c_j$ functional coefficients are null, except the $Q^\star$ variable one. From the structure of $[\alpha]$ in (8), the normality law in (6.i) is verified setting $\lambda_{it} = \frac{y_{it}}{S_{it}}$ for each triangle;
- the coefficient $c_j$ of the $Q^\star$ variable equals 1.0; then $\{u\}^T\{\beta\} = q = 1.0 = q^d$, as $Q^\star$ does not have to verify any criterion conditions: the kinematic loading condition is verified with $q^d = 1$.

Symmetry and boundary velocity conditions are enforced as detailed in the following discontinuous case.

### *3.2. Case of the virtual discontinuous velocity field*

According to [11] and [12], a discontinuity surface element (of normale $\underline{n}$) can be assimilated to a thin area whose thickness vanishes in such a manner that the normal derivatives go to infinity but the dissipated power rate remains bounded. Then the appropriate static and kinematic variables are, respectively, the stress vector $\underline{T}^\star = (T^\star_n, T^\star_t) = (\sigma^\star_n, \sigma^\star_{nt})$ and the velocity jump vector $[\underline{u}] = ([\underline{u}_n], [\underline{u}_t])$ associated by the normality law relative to the $f_{nt}(\underline{T}^\star) = 0$ criterion.

The velocity jump $[\underline{u}]$ is defined as the velocity difference between two opposite points (of the adjacent triangles) on the discontinuity segment 1-2 (Fig. 1, right). The power rate dissipated along the segment is written, with $\mathrm{d}S = 1\,\mathrm{d}l$ here:

$$P_{\text{diss}}\big([\underline{u}]\big) = \int_{12} \pi\big([\underline{u}]\big)\,\mathrm{d}l = \int_{12} \underline{T}^\star \cdot [\underline{u}]\,\mathrm{d}l, \quad \underline{T}^\star \text{ associated to } [\underline{u}] \text{ as in (6.ii)} \tag{11}$$

Relation (11) then implies that $[\underline{u}]$ is PA anywhere along the segment 1-2. It is the case here as in the classical kinematical method: when the problem (7) is solved, $[\underline{u}]$ results PA (as $\underline{v}$ in a finite element, see above) at the ends of the segment 1-2. Then, from its linearly variation along 1-2, $[\underline{u}]$ is PA anywhere from the convex character of the set of $[\underline{u}]$ PA due to the convexity of the yield criterion (see [10]). Now, from the convexity of function $\pi([\underline{u}])$, we can upper bound the dissipated power along 1-2 by writing:

$$P_{\text{diss}}\big([\underline{u}]\big) \leqslant L_{12}\big(\pi\big([\underline{u}_1]\big) + \pi\big([\underline{u}_2]\big)\big)/2 = L_{12}\big(\big\{[u]\big\}_1^T\{T^\star\}_1 + \big\{[u]\big\}_2^T\{T^\star\}_2\big)/2 \tag{12}$$

where $L_{12}$ is the length of the segment 1-2, and $\{[\underline{u}]\}_1$ is associated with $\{T^\star\}_1$, $\{[\underline{u}]\}_2$ with $\{T^\star\}_2$. Then, to the triangular element stresses, we add a stress vector, or a stress tensor, at each extremity of the discontinuity segments. Indeed, two cases can occur:

- The function $f_{nt}$ is a priori known (as for Coulomb's criterion) or it can be analytically expressed by injecting in the initial criterion the projection condition $v_{tt} = 0$: to each end of segment 1-2 is added a *vector* $\underline{T}^\star = (\sigma_n^\star, \sigma_{nt}^\star)$, which must verify the nonlinear constraint $f_{nt}(\underline{T}^\star) \leqslant 0$.
- The function $f_{nt}$ is not known or it cannot be obtained analytically as in the case of the Gurson material studied here. The difficulty is circumvented by adding a stress *tensor* $\underline{\underline{\sigma}}$ defined in the $(\underline{n}, \underline{t})$ axes to the ends of the discontinuity segment. The rows of the [B] matrix defining $v_{tt}$ (calculated for the thin zone) vanish, enforcing the projection condition to be verified by the optimal solution. If the material is isotropic, the expression of the criterion does not change in the $(\underline{n}, \underline{t})$ axes.

Finally, the plasticity criterion is the sole 'material' information we need to use the present kinematic method. Note that the extension of the above technique in the 3D case and tetrahedron element boundaries is straightforward.

**Remarks.** The boundary conditions such as zero displacement velocity are taken into account by vanishing the corresponding rows of the $[A] = [[\alpha], -\{\beta\}]$ matrix. The case of the compression of a bar under rigid plates (see Fig. 1, left) generally assumes the existence of an interface treated as a discontinuity surface obeying the bar material criterion in the case of a perfectly rough interface, as in the tests below.

- Along AB at the bar-plate interface and in the plate, let us consider additional constant stress tensors (i.e., four tensors in the case of Fig. 1) in front of the adjacent bar triangles, and also linearly varying velocity vectors, as along a side of any bar triangle. Let $N_{ip}^\star$ be the normal stress (i.e., $\sigma_{yy}$ in the axes of Fig. 1), which is constant on the plate side $ip$. Consider also $u_{ip}$ the normal velocity along the plate side. If $np$ is the number of these interface sides of $S_{ip}$ area ($np = 4$ in Fig. 1), the present exterior power rate needed to move the plate is written, after assembly:

$$P_{\text{ext}}^\star = \sum_{ip=1}^{np} N_{ip}^\star \int_{S_{ip}} u_{ip}\,\mathrm{d}S = \{N_p^\star\}^T[\gamma_p]\{u_p\} = \{u\}^T[\gamma]\{N_p^\star\} \tag{13}$$

  where $[\gamma]$ is a constant matrix resulting from the velocity integrations, $\{N_p^\star\}$ the vector of the normal stresses in the plate, and $\{u_p\}$ is the vector collecting the normal velocities (i.e., eight $u_{ip}$ in Fig. 1).
- In a second step, we achieve the equality of the velocities $u_{ip}$ with the first $u_{1p} = -U_0 = -1.0$. This is made by condensing on the first row of $[A] = [[\alpha], -[\beta]]$ the rows associated with the following $u_{ip}$. Finally, we have also an expression of type $P_{\text{ext}}^\star = Q^\star q = u_{1p}\beta Q^\star$. The previous identification leads to $q^d = u_{1p} = -1.0$, i.e., the kinematic loading condition to be verified.
- The general case of another convex contact law (see [10] for a complete presentation) here can be taken into account by adding the yield criterion of the constitutive materials plus the contact law at each end: the normality relative to the intersection of the three PA stress domains governing the behaviour of the global interface will also be verified by the final, optimal solution.

The proposed kinematic method is rigorous and general. Moreover, it is usable when the analytic expression of the power rate or the discontinuity criterion is not available, in the 2D case and in the 3D case as well. It is also a good example of synergy between two different disciplines.

## 4. Applications

To test the method, we study the problem of a Gurson bar compressed between two perfectly rough rigid plates (Fig. 1) in plane strain. The functional to be optimized is the average normal stress $F/(2Bk)$ for a ratio $B/H = 2$. Due to the symmetries, only one quarter of the bar section is discretized. The stress tensor is constant on the triangular element; the velocity field, linearly varying inside the triangle, is defined from the three apex velocities in the discontinuous case, or from the velocities of the three nodes connected to the triangle otherwise. In the discontinuous case, extra plate velocities are added to take into account the interface between the plate and the bar, as described above.

First, we implemented the method for $f = 10^{-5}$. For this porosity rate, the Gurson criterion is a very fine approximation of the von Mises criterion in plane strain and we can control the admissible character of the solution by checking, a posteriori, the admissibility of the virtual velocity fields; here only the PA condition (incompressibility and $[u_n] = 0$) needs to be verified, other conditions being exact by construction.

After optimization using Matlab, the dual variables $\{w\}$ associated with each linear constraint determine the velocity field. In addition to the PA conditions above, the functional is computed via the volumic dissipated power rate of the von Mises material. All the computations are processed on a 2-GHz Apple Powermac G5 equipped with 4.5 Go of RAM. Each mesh is labelled $B \times H$ (for example the 32 triangle-mesh of Fig. 1 is labelled $4 \times 2$). Table 1 provides the kinematic bound for several meshes for the two cases.

In all these cases, the von Mises PA condition is checked at less than $10^{-5}$: this precision is very good, specially taking into account the interior point character of the method. The dissipated power rate is also a posteriori verified at less than $10^{-5}$. In addition, the static bound 2.4247 in [6] is to be compared to the present best kinematic bound, i.e., 2.4467. Note that the discontinuous, piecewise linearized approach in [13], using the Ben-Tal linearization (equivalent to the substitution of an exterior 256-sided polygon to the von Mises criterion) gives the kinematic values 2.47400, 2.45444, and 2.44696 for the $20 \times 10$, $40 \times 20$, $60 \times 30$ cases, respectively. Not only the method is validated, but simulating a von Mises material by a low-porosity Gurson material (even in the continuous case) seems to be useful in this problem that is well known for the so-called incompressibility locking in terms of finite element method.

For a 16% porosity Gurson material, in the *continuous* velocity case below, we can note in Table 2 that solving problem is easier, as expected from the better conditioning of the Jacobian/Hessian matrices. The static bound obtained in [6] was 1.6499, to be compared to 1.6586 obtained here as upper bound. Indeed, here there is no possibility of comparison to other kinematic methods.

Table 3 gives the corresponding results in the *discontinuous* case. These results improve the results obtained without discontinuities very little, whereas the problem sizes (and CPU times) increase greatly. They confirm that considering discontinuous velocities is not very useful when the criterion is bounded in all directions, as for the von Mises case in plane stress.

Table 1
Kinematic bounds for $f = 10^{-5}$ using the continuous and discontinuous meshes

| Size | Continuous field | | | Discontinuous field | | |
|---|---|---|---|---|---|---|
| | PA verification | Result | Time | PA verification | Result | Time |
| $20 \times 10$ | $5 \times 10^{-6}$ | 2.5137 | 27 s | $3 \times 10^{-6}$ | 2.4738 | 3 m 57 s |
| $40 \times 20$ | $1 \times 10^{-5}$ | 2.4741 | 9 m 14 s | $6 \times 10^{-5}$ | 2.4542 | 1 h 27 m |
| $60 \times 30$ | $1 \times 10^{-5}$ | 2.4599 | 57 m 35 s | $9 \times 10^{-6}$ | 2.4467 | 7 h 58 m |
| $80 \times 40$ | $2 \times 10^{-5}$ | 2.4526 | 3 h 15 m 31 s | / | / | / |

Table 2
Kinematic bounds for $f = 0.16$ using the continuous mesh

| Mesh | Variables | Linear const. | Convex const. | Result | Time |
|---|---|---|---|---|---|
| $20 \times 10$ | 2403 | 790 | 801 | 1.6779 | 8 s |
| $40 \times 20$ | 9603 | 3180 | 3201 | 1.6655 | 4 m 35 s |
| $60 \times 30$ | 21 603 | 7170 | 7201 | 1.6611 | 30 m 28 s |
| $80 \times 40$ | 38 403 | 12 760 | 12 801 | 1.6586 | 1 h 32 m |

Table 3
Kinematic bounds for $f = 0.16$ using the discontinuous mesh

| Size | Variables | Linear const. | Convex const. | Result | Time |
|---|---|---|---|---|---|
| $20 \times 10$ | 9600 | 4741 | 3200 | 1.6681 | 4 m 9 s |
| $40 \times 20$ | 38 400 | 19 081 | 12 800 | 1.6606 | 1 h 22 m |
| $60 \times 30$ | 86 400 | 43 021 | 28 800 | 1.6578 | 7 h 21 m |
| $80 \times 40$ | 153 600 | 76 561 | 51 200 | / | >19 h |

## 5. Concluding remarks

Associating of the kinematic theorem of limit analysis and the interior point optimization for nonlinear constraints makes it possible to determine the kinematic bound of a problem from stress fields as variables. This association has allowed to clearly explicit the method and to solve the problem of a von Mises and Gurson infinite bar compressed under rough rigid plates. Assuming a continuous or discontinuous virtual velocity field, the method appears to be efficient and general, needing only the yield criterion as information on the material. An extension of this work to the discontinuous quadratic velocity fields, also based on convexity properties but too long to be presented here, is currently operational.

## Acknowledgements

The authors are grateful to Scott Sloan for sending them the paper [9] as a private communication, inciting them to reread the pioneering work [8]: this is the starting point of the present work. A special thanks also to S. Turgeman for pointing out a difficulty in using the kinematic theorem of LA, leading us to formulate the presentation in terms of virtual power theorem (5).

## References

[1] A.L. Gurson, Continuum theory of ductile rupture by void nucleation growth—part I: yield criteria and flow rules for porous ductile media, ASME J. Engrg. Mater. Technol. 99 (1977) 2–15.
[2] M. Trillat, J. Pastor, P. Francescato, Yield criterion for porous media with spherical voids, Mech. Res. Comm. 33 (3) (2006) 320–328.
[3] A. Ben-Tal, A. Nemirovskii, Lectures on Modern Convex Optimization. Analysis, Algorithms and Engineering Applications, Series on Optimization, SIAM-MPS, 2001.
[4] J.P. Vial, Computational experience with a primal-dual interior-point method for smooth convex programming, Optim. Methods Software 3 (4) (1994) 285–310.
[5] F. Pastor, Résolution d'un problème d'optimisation à contraintes linéaires et quadratiques par une méthode de point intérieur : application à l'analyse limite, Mémoire de DEA en mathématiques appliquées, Université de Lille 1, 2001.
[6] F. Pastor, E. Loute, Solving limit analysis problems: an interior-point method, Commun. Numer. Meth. Engrg. 21 (11) (2005) 631–642.
[7] F. Pastor, E. Loute, J. Pastor, Limit analysis and convex optimization: applications, in: 17ème Congrès Français de Mécanique—CFM 2005, Troyes, 2005.
[8] E. Anderheggen, H. Knopfel, Finite element limit analysis using linear programming, Int. J. Solids Structures 8 (1972) 1413–1431.
[9] K. Krabbenhoft, A.V. Lyamin, M. Hijaj, S.W. Sloan, A new discontinuous upper bound limit analysis formulation, Int. J. Num. Meth. Engrg. 63 (2005) 1069–1088.
[10] J. Salençon, Théorie de la plasticité pour les applications à la mécanique des sols, Eyrolles, Paris, 1974.
[11] J. Pastor, Application de la théorie de l'analyse limite aux milieux isotropes et orthotropes de revolution, Thèse d'Etat, UJF-INPG, Grenoble, 1983.
[12] J. Salençon, Calcul à la rupture et analyse limite, Presses des Ponts et Chaussées, Paris, 1983.
[13] J. Pastor, P. Francescato, M. Trillat, E. Loute, G. Rousselier, Ductile failure of cylindrically porous materials. Part 2: Other cases of symmetry, Eur. J. Mech. A/Solids 23 (2004) 191–201.